Advances in Water Resources 154 (2021) 103949

Contents lists available at ScienceDirect

Advances in Water Resources

journal homepage: www.elsevier.com/locate/advwatres

The role of hydrology on enhanced weathering for carbon sequestration II. From hydroclimatic scenarios to carbon-sequestration efficiencies

Giuseppe Cipolla [a,*], Salvatore Calabrese [b], Leonardo Valerio Noto [a], Amilcare Porporato [c]

[a] Dipartimento di Ingegneria, Universitá degli Studi di Palermo, Palermo, Italy
[b] Department of Biological and Agricultural Engineering, Texas A&M University, College Station, TX, USA
[c] Department of Civil and Environmental Engineering, Princeton University, Princeton, NJ, USA

ARTICLE INFO

Keywords:
Enhanced Weathering
Carbon Sequestration
Hydrology

ABSTRACT

Enhanced weathering (EW) scenarios are analyzed using the model presented in Cipolla et al. (2020). We explore the role of different hydroclimatic forcing on carbon-sequestration efficiencies. We also investigate whether increasing soil carbon content improves weathering conditions. We link olivine weathering rates to pH variations and quantify the suitability of hydroclimatic regimes to EW, based on rainfall intensity and frequency. The results show that the amount of CO_2 reacting with olivine and ending up in solution in the form of HCO_3^- and CO_3^{2-} increases with mean annual precipitation (MAP) up to 2000 mm, but then tapers off for higher MAPs. On the contrary, the sequestered CO_2 continues to grow with MAP in a more significant way. We also quantify the increase of nutrients availability, especially when MAP exceeds 2000 mm. Lastly, the results suggest that organic matter amendments are more effective in humid environments (MAP higher than 2000 mm), confirming the central role of hydrologic processes on EW.

1. Introduction

EW is a negative emission technology (Hegerl et al., 2015) with great potential to sequester CO_2 (Hartmann et al., 2013; Taylor et al., 2017). This strategy is based on increasing the rate of chemical weathering, a chemical/biochemical reaction that naturally occurs in soils and bedrocks. Higher rates are achieved by adding crushed silicate minerals, with higher reactive surface area than naturally occurring minerals. The weathering rates of these minerals, however, are also affected by local hydrologic processes (i.e., soil moisture dynamics), plants, soil organic matter dynamics and soil pH (Hartmann et al., 2013; Weil and Brady, 2017), a fact that complicates the estimates of the actual efficiency of EW.

Mathematical models are needed in conjunction with experiments to elucidate the interactions between soil chemistry, plants, and olivine dissolution, and predict weathering rates under variable environmental conditions. Towards this goal, in a companion paper Cipolla et al., (2021) we developed a model coupling soil biogeochemical processes (pH, CO_2, cation exchange) and ecohydrological dynamics (soil moisture, plants) to the dissolution of olivine in the soil root zone. The model allows us to explore the role of precipitation (hereafter named 'climate effect') and its intermittency, plants and other ecohydrologic processes, as well as biogeochemistry on EW dynamics.

In this paper, we employ detailed model simulations to answer the following questions: which climates are more suitable to EW? What are the rates of CO_2 sequestration resulting from olivine dissolution for given climate and land use conditions, including the presence of soil organic matter? What is the order-of-magnitude of the nutrients increase in soil water due to olivine dissolution?

The main motivation that inspired this work is to quantify the role of hydrological processes on EW dynamics. Indeed, characterizing various climate conditions with respect to EW could help decision makers to define the parts of the globe more suitable for amending soil with reactive minerals, in perspective to put EW into practice. To the best of our knowledge, the actual rates of CO_2 sequestration due to olivine dissolution in the field are not well defined, as many studies (Hartmann et al., 2013; Renforth et al., 2015; ten Berge et al., 2012) base their estimates on the theoretical limit of 1.25 g_{CO_2}/g_{oliv}. To this regard, our model allows to better characterize the actual rates of CO_2 sequestration, considering the dynamics of bicarbonate (HCO_3^-) and carbonate (CO_3^{2-}) ions in soil water resulting from olivine dissolution. We also investigate whether we can improve EW by amending soil with organic matter, since this can lead to a change in soil chemistry (i.e., cation exchange and pH) and, in turn, weathering rates. Another goal is related to quantify the increase of nutrients availability and pH, as also noted by Weil and Brady (2017) and Renforth et al. (2015), due to olivine dissolution since, in some cases, these aspects can enhance plants productivity (Atkinson et al., 2010).

* Corresponding author.

https://doi.org/10.1016/j.advwatres.2021.103949
Received 11 May 2021; Accepted 11 May 2021
Available online 25 May 2021

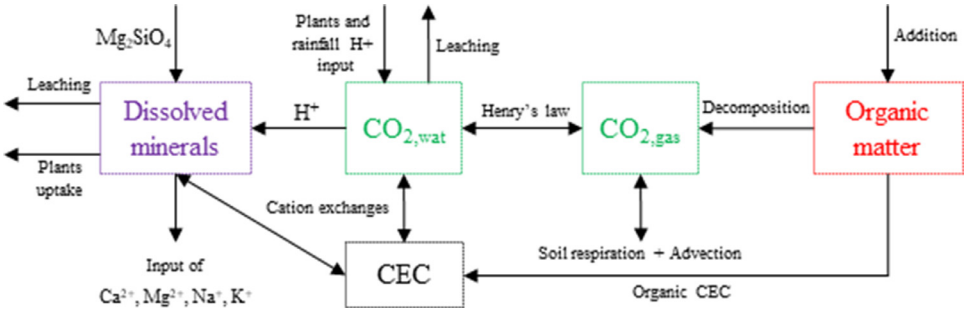

Fig. 1. Flow chart of the main involved mass fluxes among the components of the model in olivine weathering process. This figure is a simplified version of Fig. 2 in Cipolla et al. (2020).

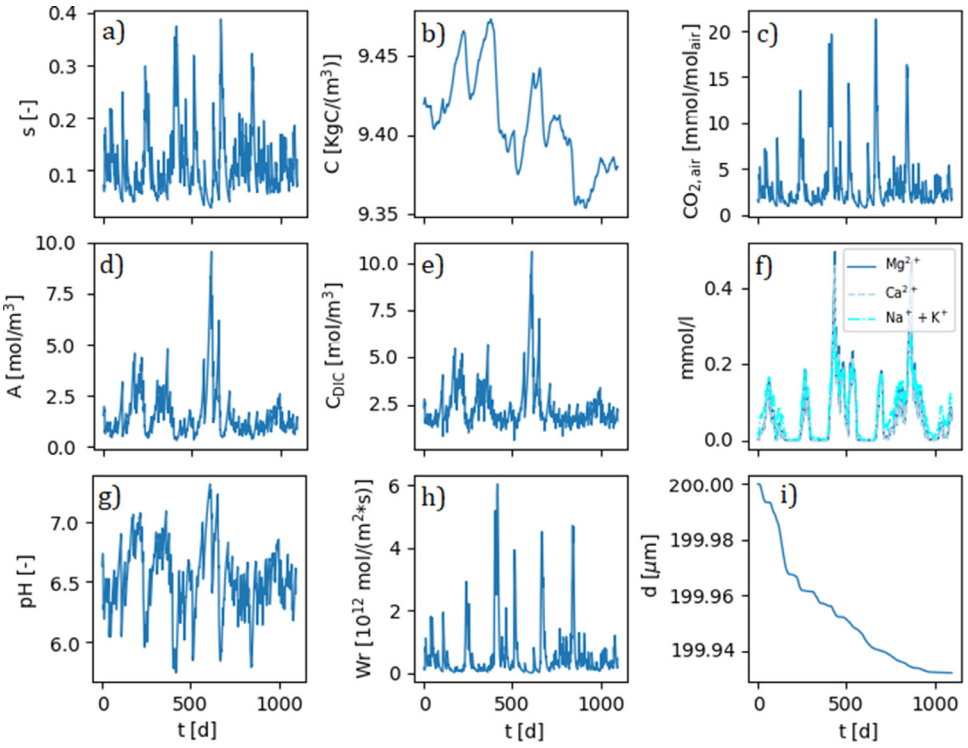

Fig. 2. Time series of the most representative variables of the model after running a generic simulation of the model by means of the parameters of the S1 scenario, listed in Table 1. Panels display the time-series of: (a) soil moisture, (b) organic matter concentration, (c) CO_2 concentration in the gas phase, (d) alkalinity, (e) total dissolved inorganic carbon concentration, (f) Mg^{2+}, Ca^2+ and the sum of Na^+ and K^+ concentrations, (g) pH, (h) weathering rate and (i) the reduction of olivine particles diameter.

The structure of the paper is as follows: Section 2 gives a brief description of the model, of its parameters and some used data to carry out the applications. In this section a description of different simulation scenarios is also provided. In Section 3, we address the research questions by analyzing and discussing the results. Finally, Section 4 provides some conclusions.

2. Materials and methods

2.1. Model overview

The model (Cipolla et al., 2020) takes into account the fundamental interactions among ecohydrological (e.g., plants, water, nutrients) and biogeochemical (e.g., pH, CEC) processes driving mineral dissolution. The external forces of the model can be either precipitation measurements or stochastic rainfall time-series for long term simulations. On the bases of the involved mass fluxes among the components of the model, represented in Fig. 1 it is possible to write the related differential equations describing the mass balance and the chemical reactions of the involved elements.

The model simultaneously simulates the balance of soil organic carbon, which is one of the CO_2 sources in the system, the dynamics of CO_2 in the gas phase and of the part of it that reacts with water, the dynamics of dissolved elements that do not contain carbon; these include plant nutrients and the products of olivine dissolution (i.e., silicates and Mg^{2+}) and the cation exchange capacity, representative of the equilibrium exchanges between soil organic and inorganic colloids and the dissolved ions.

The model is summarized by a system of eight mass balance differential equations, representative of the temporal dynamics of eight state variables, namely: the total carbon in the system ($C_t = [CO_{2,air}] + C_{DIC}$, where $C_{DIC} = [H_2CO_3^*] + [HCO_3^-] + [CO_3^{2-}]$), the total alkalinity ($A_t = C_{DIC}(\alpha_1 + 2\alpha_2) - [H_t^+] - 3[Al^{3+}{}_t] + [OH^-]$, where

Table 1
List of parameters varying among the different climate scenarios.

Parameter	Value				
Scenario	S1	S2	S3	S4	S5
λ [d^{-1}]	0.23	0.33	0.5	0.63	0.75
MAP [mm]	920	1325	2010	2530	3010
ADD [gC m^{-2}d^{-1}]	1.5	1.8	2.2	2.5	2.7
T_{max} [mm d^{-1}]	4.5	5.1	6	6.8	7.3
$I_{Ca^{2+}}$ [μmolm^{-2}d^{-1}]	100	200	300	400	500
$I_{Mg^{2+}}$ [kg ha^{-1}y^{-1}]	1.1	1.36	1.78	2.1	2.4
I_{K^+} [kg ha^{-1}y^{-1}]	0.5	1	1.5	2	2.5
I_{Na^+} [mg m^{-2}d^{-1}]	3	4.6	7	9	10

$H_t^+ = H^+ + x_{H^+_{OM}} + x_{H^+_{clay}}$), the total masses of calcium ($Ca_t^{2+} = Ca^{2+} + x_{Ca^{2+}_{OM}} + x_{Ca^{2+}_{clay}}$), magnesium ($Mg_t^{2+} = Mg^{2+} + x_{Mg^{2+}_{OM}} + x_{Mg^{2+}_{clay}}$), sodium ($Na_t^+ = Na^+ + x_{Na^+_{OM}} + x_{Na^+_{clay}}$), potassium ($K^+{}_t = K^+ + x_{K^+{}_{OM}} + x_{K^+{}_{clay}}$) and aluminum ($Al^{3+}{}_t = Al^{3+} + x_{Al^{3+}{}_{OM}} + x_{Al^{3+}{}_{clay}}$) and the total silicon in the system ($Si_t = H_2SiO_3 + HSiO_3^- + SiO_3^{2-}$).

$$\begin{cases} \frac{dC_t}{dt} = rDEC - F_s - ADV - L_{C_{DIC}} \\ \frac{dA_t}{dt} = -L_{HCO_3^-} - 2L_{CO_3^{2-}} - RI - PI + L_{H^+} + \\ -L_{OH^-} + W_{bg} + 4W_{oliv} - 3I_{Al^{3+}} + 3L_{Al^{3+}} \\ \frac{dCa_t^{2+}}{dt} = I_{Ca^{2+}} - L_{Ca^{2+}} - UP_{Ca^{2+}} \\ \frac{dMg_t^{2+}}{dt} = I_{Mg^{2+}} - L_{Mg^{2+}} - UP_{Mg^{2+}} + 2W_{oliv} \\ \frac{dNa_t^+}{dt} = I_{Na^+} - L_{Na^+} - UP_{Na^+} \\ \frac{dK_t^+}{dt} = I_{K^+} - L_{K^+} - UP_{K^+} \\ \frac{dAl_t^{3+}}{dt} = I_{Al^{3+}} - L_{Al^{3+}} \\ \frac{dSi_t}{dt} = -L_{Si_t} + W_{oliv} \end{cases} \quad (1)$$

We refer to Cipolla et al. (2020) for details. The system of Eq. (1) is solved with a time explicit forward scheme, fixing the initial conditions for $C_t, A_t, Ca_t^{2+}, Na_t^+, Mg_t^{2+}, K_t^+, Al_t^{3+}$ and Si_t. To derive the concentration of the considered dissolved ions ($H^+, Na^+, Ca^{2+}, Mg^{2+}, K^+ Al^{3+}$) or other individual variables, it is necessary to solve an implicit algebraic system with twenty two algebraic equations in as many unknown terms (see Cipolla et al. (2020) for details). The temporal dynamics of the total carbon is a function of the carbon decomposition rate (DEC), the CO_2 released to the atmosphere due to soil respiration (F_s), the advection flux of CO_2(ADV), namely the CO_2 entering the soil during the drying process and out of the soil during the wetting process, and the amount of $H_2CO_3^*, HCO_3^-$ and CO_3^{2-} transported out of the root zone by leaching ($L_{C_{DIC}}$). The change of the total alkalinity over time is related to the leaching of dissolved ions ($HCO_3^-, CO_3^{2-}, H^+, OH^-$and Al^{3+}), the input of H^+ due to the infiltration rate (RI), the input of H^+ from vegetation (PI), the background weathering, representative of the H^+ losses due to naturally present minerals, excluding olivine, in the soil (W_{bg}), the H^+ losses due to olivine dissolution (W_{oliv}) and the input of Al^{3+} in the system ($I_{Al^{3+}}$). The time dynamics of the total calcium, magnesium, sodium and potassium depend on an input term, including the atmospheric deposition, the return of cations from plant litter and an input from minerals dissolution ($I_{Ca^{2+}}, I_{Mg^{2+}}, I_{Na^+}$ and I_{K^+}), the losses by leaching ($L_{Ca^{2+}}, L_{Mg^{2+}}, L_{Na^+}$ and L_{K^+}) and plant uptake ($UP_{Ca^{2+}}, UP_{Mg^{2+}}, UP_{Na^+}$ and UP_{K^+}) and, only for magnesium, an additional input due to the weathering of olivine (W_{oliv}). The temporal dynamics of aluminum, instead, are only regulated by an input due to the dissolution of parent materials ($I_{Al^{3+}}$) and a loss by leaching ($L_{Al^{3+}}$). Lastly, the variation of the total silicon over time depends on the input from olivine dissolution (W_{oliv}) and the output due to leaching (L_{Si_t}).

In the simulations we paid particular attention to the temporal dynamics of soil water pH, both with and without olivine, since this has an impact on several other processes, including the dissolved ions concentration dynamics and the suitability of the environment for plants. It can be further considered as a proxy for assessing the amount of sequestered carbon from a certain mass of olivine, as reported by the analyses conducted in this work.

2.2. EW scenarios

To assess the role of climate on EW and explore solutions aimed to enhance weathering rates and carbon sequestration, we simulated the dissolution of olivine under different mean annual precipitation (MAP) scenarios. We explored five scenarios, labeled S1 to S5, characterized by the same average rainfall depth (α), but different storm frequencies (λ), resulting in MAP ranging from about 900 to 3000 mm (details in Table 1). We focused on this range because, for MAP lower than 900 mm, the environment is too dry for EW applications (Weil and Brady, 2017), while only a limited area of the globe has MAP higher than 3000 mm. Since we are interested in the role of climate on EW, we maintained soil and vegetation properties constant. For the sake of simplicity, we did not carry out our analyses with reference to a forested soil, in order to neglect the presence of aluminum in the system that, as explained in Cipolla et al. (2020), would represent one of the major H^+ sources for this strong acid soil. For the background weathering, we used the dissolution rate constant of anorthite. In all scenarios, we considered the addition of 10 kg of olivine, after the soil biogeochemistry (time-series of C, and of dissolved and adsorbed Ca^2+, Mg^{2+}, K^+ and Na^+) had reached a statistically stationary regime, consistent with the given climate. The effects of olivine dissolution on soil chemistry and carbon sequestration were then analyzed after a simulated period of five years, in order to look at the short-middle term effects of olivine dissolution. We here omit the long term effects of olivine dissolution since they are not consistent with the short-middle term goals of carbon sequestration, in order to counteract the greenhouse effect. In any case, the analyses may be extended to any time horizon.

We also explored to what extent organic matter amendments (e.g., compost) would increase weathering rates and carbon sequestration. We simulated organic matter amendment by increasing the soil carbon input (ADD) in all scenarios by 0.2 gC $m^{-2}d^{-1}$ (Table 1), or equivalently 73 gC $m^{-2}y^{-1}$. On the basis of the amount of extractable organic carbon of grass cuttings (Baca et al., 1996) (about 25 g_{OC} $kg^{-1}_{compost}$), this amount would correspond to 3 $kg_{compost}$ $m^{-2}y^{-1}$, which is the typical average amount of compost used to amend an agricultural soil. For each scenario, the effect of organic amendment is assessed by maintaining the same time-series of soil moisture as for the base scenarios without amendment to better isolate the changes in soil chemistry and carbon sequestration due to the additional organic matter.

As an example, we here present a typical model simulation, carried out with the parameters related to the S1 scenario, presented in Table 1. Fig. 2 shows the time-series of the most representative variables of the model (i.e., (a) soil moisture, (b) organic matter concentration, (c) CO_2 concentration in the gas phase, (d) alkalinity, (e) total dissolved inorganic carbon concentration, (f) Mg^{2+}, Ca^2+ and the sum of Na^+ and K^+ concentrations, (g) pH, (h) weathering rate and (i) the reduction of olivine particles diameter) related to a time interval of about three years after olivine addition. As soil moisture increases, there is a stronger decomposition of organic matter, a lower pH and a greater weathering rate.

2.3. Parameterization

The values for the parameters related to climate, soil, and vegetation are listed in Table 2. We consider a sandy soil for all scenarios in order to better highlight the role of climate on EW, without confounding factors deriving from different soil properties. The specific CEC of organic matter and clay colloids are extracted from Weil and Brady (2017), while the selectivity constants, related to the CEC, from Suarez and Ŝimunek (1997).

The values of ADD, the maximum transpiration rate and the input of calcium, magnesium, potassium and sodium for the five considered climate scenarios are reported in Table 1. We used typical levels of input of calcium, magnesium, potassium and sodium provided by Pulido-Villena et al. (2006), Groshans et al. (2019), Mikhailova et al. (2019) and Suweis et al. (2010), which scale according to MAP, based on the observation that deposition increases with MAP (Pulido-Villena et al., 2006; Groshans et al., 2019; Mikhailova et al., 2019). The mass fraction of anorthite is representative of all the minerals within the soil, different than olivine, consuming H^+ due to their weathering processes. This parameter is fixed equal to 1%, but it could be modified in order to increase or decrease the term related to these weathering processes. The diameter of the anorthite particles was assumed to be equal to that of the olivine particles. The background weathering is fundamental to char-

Table 2
List of parameters of soil, vegetation, climate and weathering in the model.

	Symbol	Value	Reference
Soil parameters			
Porosity	n	0.4	Assumed
Soil depth	Z_r [m]	0.8	Assumed
Field capacity	s_{fc}	0.3	Assumed
Hygroscopic point	s_h	0.02	Assumed
Saturation hydraulic conductivity	K_s [m d^{-1}]	1.1	Assumed
Pore size distribution index	b	4	Assouline (2005)
Initial carbon concentration in the soil	C_{in} [gC m^{-3}]	10000	Assumed
Initial carbon concentration in the biomass	C_b [gC m^{-3}]	100	Assumed
Bulk density	ρ_b [kg m^{-3}]	1600	Zeri et al. (2018)
Specific CEC_{OM}	$CEC_{OM,s}$ [cmol kg$^{-1}_{\text{OM}}$]	200	Weil and Brady (2017)
Specific CEC_{clay}	$CEC_{clay,s}$ [cmol kg$^{-1}_{\text{clay}}$]	80	Weil and Brady (2017)
Mass fraction of clay	f_{clay}	0.1	Zeri et al. (2018)
Selectivity constant $Ca^{2+} - Mg^{2+}$ for OM	$SC_{OM}(Ca^{2+} - Mg^{2+})$	4.65	Suarez and Šimunek (1997)
Selectivity constant $Ca^{2+} - Mg^{2+}$ for clay	$SC_{clay}(Ca^{2+} - Mg^{2+})$	1.1	Suarez and Šimunek (1997)
Selectivity constant $Na^{+} - Ca^{2+}$ for OM	$SC_{OM}(Na^{+} - Ca^{2+})$	10	Suarez and Šimunek (1997)
Selectivity constant $Na^{+} - Ca^{2+}$ for clay	$SC_{clay}(Na^{+} - Ca^{2+})$	1.96	Suarez and Šimunek (1997)
Soil-vegetation parameters			
Point of incipient stress	s^*	0.17	Assumed
Permanent wilting point	s_w	0.065	Assumed
Vegetation parameters			
Evaporation at the wilting point	E_w [mm d^{-1}]	1	Assumed
Carbon decomposition parameters			
Decomposition constant	k_{dec} [m^{3}d^{-1}gC^{-1}]	6.5×10^{-6}	Assumed
Carbon respiration fraction	r	0.7	Porporato et al. (2003)
Rainfall parameters			
Average storm depth	α [mm]	11	Assumed
CO_2 parameters			
Atmospheric CO_2 concentration	$CO_{2_{atm}}$ [ppm]	412	Assumed
Free-air diffusion coefficient of CO_2	D_0 [m^{2}s^{-1}]	1.6×10^{-5}	Riley et al. (2011)
Background weathering parameters			
Specific dissolution rate of anorthite	k_{bg} [mol m^{-2}s^{-1}]	5.6×10^{-9}	Lasaga (1984)
Diameter of anorthite particles	d_{bg} [μm]	200	Assumed
Mass fraction of anorthite	f_{bg}	0.01	Assumed
Density of anorthite	ρ_{bg} [g cm^{-3}]	2.75	Mueller et al. (2005)
Olivine weathering parameters			
Specific dissolution rate	k_{sil} [mol m^{-2}s^{-1}]	1×10^{-10}	Lasaga (1984); Renforth et al. (2015)
Dissolution constant	$Log(k_{eq})$	7.11	Morel and Hering (1993)
Molar volume	V_M [cm^{3}mol^{-1}]	44.08	ten Berge et al. (2012)
Effective diameter of particles	ϕ[μm]	200	Renforth et al. (2015)
Density	$\rho_{oliv}[gcm^{-3}]$	3.275	Ahrens et al. (1971)
Mass of added olivine	$M_{oliv}[kg_{\text{olivine}}m^{-2}]$	10	Renforth et al. (2015)

acterize the initial soil pH, consistently with the given climate. Indeed, this strongly affects olivine dissolution dynamics. In this paper, anyway, the background weathering characteristics (i.e., the mass fraction and diameter of anorthite particles) are considered constant among the five analyzed climate scenarios, mainly due to the fact that the main goal of the study is to explore the climate effects on EW. Therefore, in order to isolate these effects, all the soil and vegetation parameters do not have to vary with respect to MAP. It is however worth noticing that for case-study applications the background weathering parameters should be defined based on the soil properties under analysis. Olivine amendment is set to 10 kg_{olivine} m^{-2}, approximately equal to the amount used in the pot experiment by Renforth et al. (2015) (the authors used 100 g of olivine for a cylindrical soil sample of diameter 0.1 m and height 1 m, corresponding to about 12 kg_{olivine} m^{-2}).

Plant biomass productivity is positively correlated to MAP, especially when this is higher than 600 mm (Porporato and Rodriguez-Iturbe, 2013). To take this aspect into account, we rescaled the input of organic matter from plant litter (*ADD*) (Porporato et al., 2003) according to the annual plant productivity of the given climate. The increase of the MAP and plant biomass productivity also leads to a higher transpiration rate. Generally transpiration rate is linearly related to the canopy cover (Pelak et al., 2017), which likely increases as the plant biomass productivity grows. We thus rescaled the maximum transpiration rate according to MAP, also based on typical values of potential evapotranspiration at the global scale (Weiß and Menzel, 2008).

3. Results and discussion

3.1. Climate effects

Climate mainly affects the dissolution of olivine and CO_2 sequestration through its control on the soil moisture dynamics. The latter in fact affects organic carbon decomposition, soil pH, and in turn olivine dissolution and leaching of dissolution products. While in the next section a comparison between the dynamics under a dry (S1) and a wet (S5) scenarios is carried out, in the Sections 3.2 and 3.3 we then analyze the results provided by all five scenarios.

3.1.1. Temporal dynamics of soil moisture and organic carbon

The time series of soil moisture and organic carbon for the S1 and S5 scenarios (see Table 1) are presented in Fig. 3a and b, respectively, along with the probability distribution functions (pdfs) of soil moisture. As expected, while the soil water content under the S5 is on average higher than that of S1 (an average of 0.26 in S5 and 0.11 in S1), the figure also shows that in the former there is higher variability, as evident from the standard deviation (0.13 in S5 and 0.06 in S1) and more in general from the pdfs shape. The propagation of soil-moisture variability to the organic carbon depends on the inertia of the organic matter pool, represented by the decomposition constant, k_{dec}, and the carbon concentration in the biomass pool, C_b, as described in Porporato et al. (2003) and D'Odorico et al. (2003). Overall, although the carbon

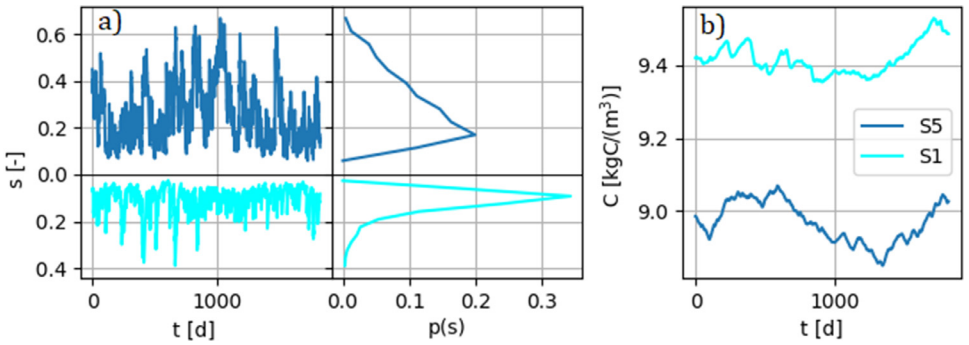

Fig. 3. Time series of soil moisture (a) and organic carbon (b) in the S1 and S5 scenarios. In Fig. 3a the empirical pdfs of soil moisture under the S1 and S5 scenarios are also displayed. Panel (a) presents a reflected axis, thus the values in the lower half are positive.

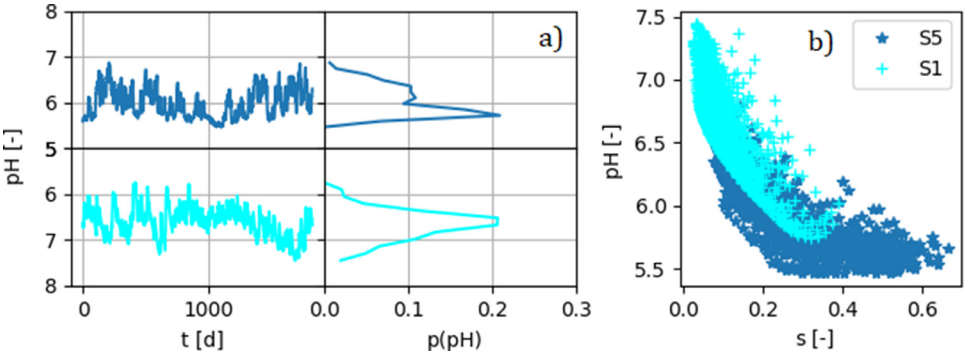

Fig. 4. Time series of soil pH (a) and soil pH vs soil moisture (b) in the S1 and S5 scenarios. In Fig. 4a the empirical pdfs of pH under the S1 and S5 scenarios are also displayed. The visualization scheme is the same to that in Fig. 3.

input is higher in wetter climates (Table 1), the organic carbon mean concentration is higher in scenario S1 (9.4 kgC m^{-3}) than S5 (8.8 kgC m^{-3}), as the effect of faster decomposition prevails; indeed, wet environments are generally more suitable for the biomass to decompose the organic matter, since microbial activity and consequently the decomposition rates are higher (D'Odorico et al., 2003,1973). Scenario S1 also has higher standard deviation, which is explained by the inverse proportionality between decomposition and soil moisture when the latter is above field capacity.

3.1.2. pH-soil moisture relation

Since in both simulations the same soil properties are considered, the differences in pH dynamics are only due to a different soil water content and a different organic matter concentration, which depends on the carbon input and decomposition rate. In agreement with observations, which report that, at a global scale, soils are more acidic in humid climates (Slessarev et al., 2016; Merry, 2009), in our scenarios soil pH is generally higher in S1 (6.6 on average) than in S5 (5.9 on average) (Fig. 4a). These pH levels are also in line with typical pH values found in wet and dry environments, respectively (see Fig. 3a in Slessarev et al. (2016) or Merry (2009)). This tendency originates from multiple factors; one is related to the amount of H^+ in rainfall. In fact, because of slight acidity of normal rain, soils in regions with higher MAP receive more H^+. Furthermore, as plants uptake nutrients from soil water, such as Ca^2+, Mg^{2+}, K^+ and Na^+, that are positively charged, they release H^+ ions to balance the extra-uptake of positively charged ions and maintain a neutral charge. This is favored in wetter climates with higher plant water and nutrient uptake rates. Lastly, due to the low leaching, dry soils tend to accumulate alkaline ions, such as carbonate and bicarbonate ions, mainly generated from the organic matter decomposition, that can react with H^+ and help maintain higher soil pH.

Looking at the probability density functions (pdfs) it is also evident that scenario S5 presents a slightly higher variability, as confirmed by the standard deviation values (0.32 in S5 and 0.30 in S1). By looking at its pdf we notice the presence of a double peak and that, especially when the pH is high, it tends to remain at this level for a certain amount of time before decreasing. A high pH is associated to low soil moisture values (see Fig. 4b) and, consequently, given the low decomposition rate, to high concentrations of organic carbon. This leads to a high organic CEC, and thus to a strong buffering capacity and resistance to pH variations. Therefore, in these conditions, the CEC tends to keep the pH high, until soil moisture and decomposition rate of organic matter increase in a significant way, resulting in a reduction of CEC and therefore in a lowering of pH. The repeating occurrence of such phenomena leads to the presence of a peak in the pdf even at higher pH (specifically at pH of about 6.3), apart from the most probable pH in S5 scenario, which is about 5.8. This aspect is not visible in the S1 scenario, since it is characterized by a lower pH and smaller soil moisture variability, and hence there are not abrupt changes in the soil buffering capacity and pH, which tends to be concentrated around the most probable value (equal to about 6.7).

3.1.3. Olivine dissolution dynamics

The effect of climate on olivine-dissolution dynamics can be clearly seen on the different temporal evolution of the weathering rate (Fig. 5a), the latter being one order of magnitude higher in scenario S5 (wetter) than S1. In particular, the mean weathering rate is 4.3×10^{-12} mol $m^{-2}s^{-1}$ in S5 and 4.6×10^{-13} mol $m^{-2}s^{-1}$ in S1. This is not a surprising result, since previous studies already observed that higher soil water content leads to higher reactive surface areas of olivine particles and, in turn, to higher dissolution rates (Weil and Brady, 2017; Sverdrup and Warfvinge, 1988; Hartmann et al., 2013).

The relation between weathering rate and soil moisture reflects the number of interactions involved in the olivine dissolution dynamics. As it clearly appears from Fig. 6a, even if the direct influence of soil moisture on weathering rate is assumed linear (linear soil moisture - mineral surface area relation), the effective relationship, that also takes into account the indirect influence of soil moisture, results in a non-linear and non-unique relationship. Indirect effects include for instance the role of soil moisture variability on pH, which, in turn, is another important variable affecting the weathering rate ((Hartmann et al., 2013; Weil and Brady, 2017)). Figure 6a also highlights that weathering rate and soil moisture exhibit interesting hysteresis cycles, with lower weathering rates during the wetting process and the higher ones during the drying phase.

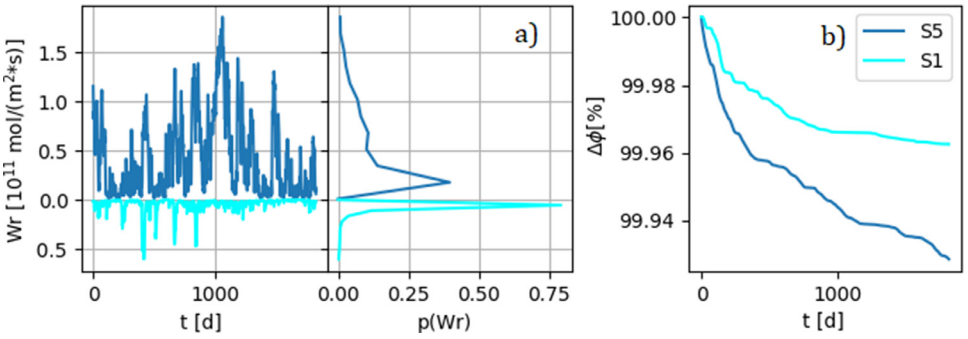

Fig. 5. Time series of olivine weathering rates and their empirical pdfs (a); variation of the particles diameter over time under the S1 and S5 scenarios (b). The visualization scheme is the same to that in Fig. 3.

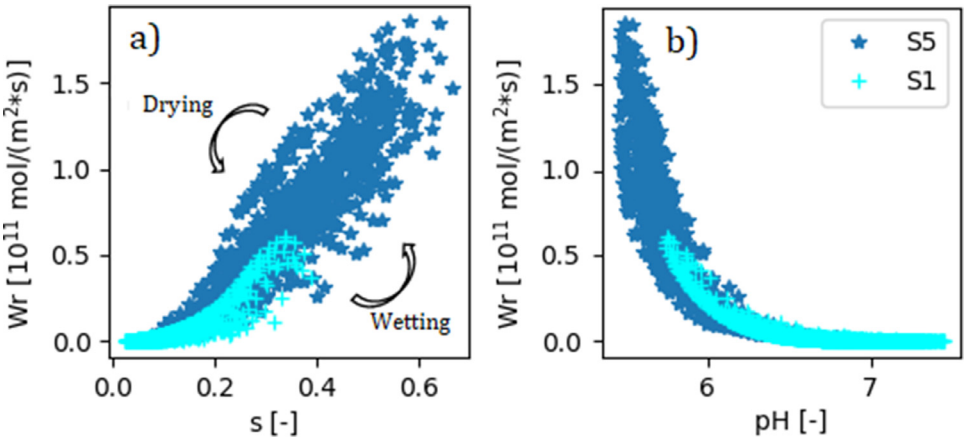

Fig. 6. Pattern of olivine weathering rate with soil moisture (a) and with soil pH (b) under the S1 and S5 scenarios.

Although olivine has one of the highest dissolution rates compared to other minerals (Hartmann et al., 2013), the dissolution times are relatively long, regardless of soil moisture and pH conditions. Indeed, according to Lasaga (1984) the mean lifetime of a 1 mm diameter olivine particle is equal to about 600,000 years. This is confirmed in Fig. 5b where, even at high MAP, five years after the addition of olivine, the diameter reduction is very low (e.g., about 0.06 % for the S5 scenario). In any case, the effect of different climates in the reduction of the diameter of olivine particles is evident since, under the S5 scenario, it is greater than that of the S1 scenario, due to the generally higher weathering rate.

3.2. The role of organic matter on EW

As we have seen above, the olivine weathering rate increases as soil water becomes more acidic. To this regard, it is interesting to explore whether increasing the organic matter content by means of soil amendment can increase the availability of H^+ for olivine dissolution and, in turn, increase weathering rate. Fig. 7 compares, in a box-plot form, the organic carbon concentration (Fig. 7a), soil pH (Fig. 7b) and olivine weathering rate (Fig. 7c) achieved with and without carbon amendment. The effects of organic matter amendment are evaluated for a period of 5 years after the addition of olivine for all climatic scenarios.

The changes in the organic carbon concentration mainly depend on how much the decomposition term grows relative to the addition itself. The decomposition rate is linearly related to the organic carbon concentration, which is generally expected to grow if the carbon input is higher. Our results show that, due to a higher decomposition rate, the organic carbon tends to decrease with MAP, especially when it exceeds 1300 mm. A similar pattern is visible under the scenario with carbon amendment, even though, as expected, with higher values of carbon concentration. While this relation may appear to contradict global scale observations of soil organic carbon, we emphasize that the maximum variation of organic matter between the driest and the wettest scenario is very small (only about 2 kg_C m^{-3}). In the analysis, we also considered

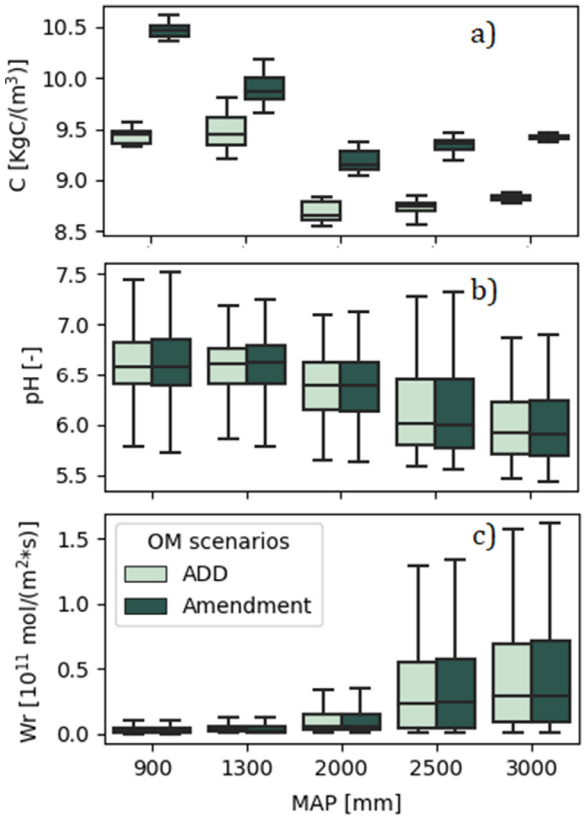

Fig. 7. Box plots for the organic carbon concentration (a), soil pH (b) and olivine weathering rate (c) under all the considered climate scenarios and two different inputs of organic matter.

constant soil properties and composition, a fact that may considerably affect organic matter decomposition dynamics.

The pH tends to decrease with MAP under both the carbon input scenarios. This extends the result reported in figure 4a to all the considered climate scenarios. It is also relevant to see that, as MAP increases, the soil pH at the scenario with carbon amendment progressively gets close to the one related to the base carbon input in Table 1 until, in very humid conditions, which are provided by a MAP greater than 2000 mm, the higher carbon input leads to a slight reduction of soil pH. With reference to the pH variability, there seems to be no pattern with MAP and, under the amendment scenario, the interquartile range is almost the same as in the case where the increase of organic matter is not considered. We can thus conclude that organic matter amendment is effective under very humid climates, where it leads to a pH reduction.

In general, the response of pH to the increase of organic matter depends on a balance between two contrasting effects: the increase of soil buffering capacity and the greater decomposition of carbonate and bicarbonate ions along with the greater input of H^+ due to infiltration and plants action. On the one hand, in dry conditions, a greater pH is recorded under higher organic matter addition, because the increase in the organic CEC, and thus of the soil buffering capacity, prevails over the plant and rainfall input of H^+. On the other hand, in wet conditions, the input of H^+ due to infiltration and plants action tends to become more relevant than the increase in soil buffering capacity, leading to a reduction in soil pH. Furthermore, the faster decomposition of organic matter in wet climates leads to a greater increase of the carbonic acid and bicarbonate ion concentration in the soil water, which rapidly dissociate releasing H^+ and lowering soil pH.

The variation of soil pH due to the different climate and organic matter addition scenarios affects olivine weathering rate. Whether soils are organically amended or not, there is a significant increase of the weathering rate with MAP (Fig. 7c) and its interquartile range, which is representative of the weathering rate variability. However, adding organic matter is effective only when MAP exceeds 2000 mm since, in correspondence of the carbon amendment scenario, the weathering rate is slightly greater than in the case achieved with the carbon input values presented in Table 1 (i.e., in Fig. 7c, at the 'Amendment' scenario, the median weathering rate is slightly higher than the one achieved at the 'ADD' scenario). This is a natural consequence of the pH reduction which, under the greater carbon input, only occurs when MAP exceeds 2000 mm.

3.3. Analysis of EW benefits

Several studies have shown that using olivine for EW applications leads to carbon sequestration and increase of nutrients availability (Renforth et al., 2015; Hartmann et al., 2013). Estimates of carbon sequestration (Hartmann et al., 2013; Renforth et al., 2015; ten Berge et al., 2012), however, are generally based on the theoretical limit of 1.25 g_{CO_2}/g_{oliv}, although it is acknowledged that the actual sequestration can be considerably lower and time varying. To this regard, our model allows us to finalize such estimates, for example by taking into account the effect of extra amount of bicarbonate (HCO_3^-) and carbonate (CO_3^{2-}) ions in soil water originating from olivine dissolution and in relation to whether they are transported away to groundwater and to stream through soil water percolation.

This distinction is particularly important since HCO_3^- and CO_3^{2-} ions in soil water due to the weathering of olivine could potentially react with H^+ to form carbonic acid, causing an increase in pH and a consequent slow down of the olivine dissolution rate. On the contrary, actual carbon sequestration is more closely related to the extra HCO_3^- and CO_3^{2-} ions that are leached away from the soil. The actual sequestered carbon due to EW can be estimated as the leached mass of the extra HCO_3^- and CO_3^{2-} produced by olivine dissolution, at each time step.

Apart from carbon sequestration, olivine application leads to other effects related to the changes in soil chemistry. For instance, by reacting with H^+ it leads to an increase of soil pH. In many cases, this is beneficial to plant productivity (Weil and Brady, 2017; Atkinson et al., 2010), which may be further enhanced by the release of nutrients upon olivine dissolution (Renforth et al., 2015). It is worth noting that a nutrient increase in soil water is not necessarily beneficial for vegetation (in Section 3.3.2, we show the increase of nutrients in soil water as a common effect of olivine dissolution). For example, an excess of Mg^{2+} in soil water may be the cause of reduced soil fertility, which depends on the Ca:Mg ratio at the exchange sites (Kopittke and Menzies, 2007).

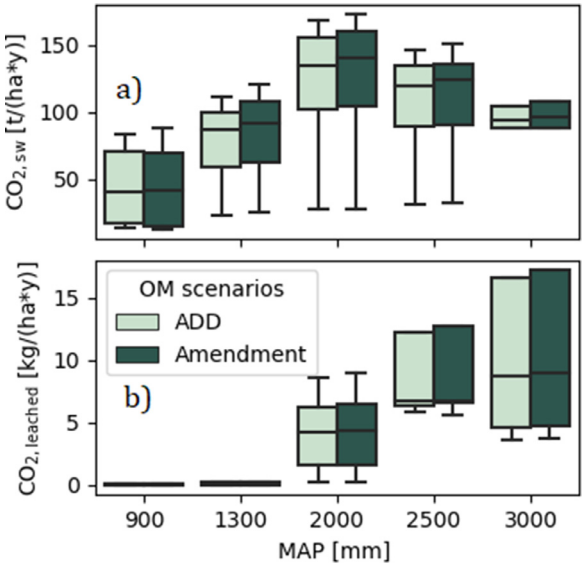

Fig. 8. Box plots of the annual mass of CO_2 that reacts with olivine and is dissolved in soil water in the form of HCO_3^- and CO_3^{2-} (a) and of the annual mass of sequestered CO_2 by leaching (b). The plots are related to all the considered climate scenarios and different inputs of organic matter.

3.3.1. Carbon sequestration

Olivine reacts with CO_2 drawing it into solution to form HCO_3^- and CO_3^{2-} ions. However, due to the reasons described in Section 3.3, the actual sequestered CO_2 is better connected to the leached mass of these ions. In Fig. 8a we plot the equivalent mass of CO_2, called $CO_{2,sw}$, assessed on the base of the carbon contained in the mass of HCO_3^- and CO_3^{2-} produced from olivine dissolution, while Fig. 8b displays a box plot of the sequestered CO_2, evaluated as a function of the leached mass of HCO_3^- and CO_3^{2-}.

The $CO_{2,sw}$ increases with MAP only up to 2000 mm (Fig. 8a), mainly due to the rapid increase in weathering rate under this MAP threshold. However, at MAP greater than 2000 mm, there is a decrease of the $CO_{2,sw}$, in spite of the weathering rate increase. This fact could be connected to the methodology used in its evaluation, which does not take into account the outputs of HCO_3^- and CO_3^{2-} ions. For instance, some HCO_3^- and CO_3^{2-} react with H^+ and form the carbonic acid. Comparing the plots related to the different carbon input scenarios, it is worth noticing that, adding organic matter seems to be effective, especially for MAP above 2000 mm, since there is a general increase of $CO_{2,sw}$.

The sequestered CO_2, instead, increases with MAP for two reasons: i) higher weathering rates imply greater concentrations of HCO_3^- and CO_3^{2-} in soil water and ii) higher MAP increasing the percolation rates. The combination of these two factors lead to an increased sequestered CO_2 with MAP at a rate which is faster than the increase in weathering rate itself. The small mass of sequestered CO_2 under all climate scenarios is due to the short time interval used in the box plots generation (i.e., five years), which does not allow us to see significant effects from the leaching component. Indeed, according to Hartmann et al. (2013), at longer time scales of decades or centuries, the cations resulting from

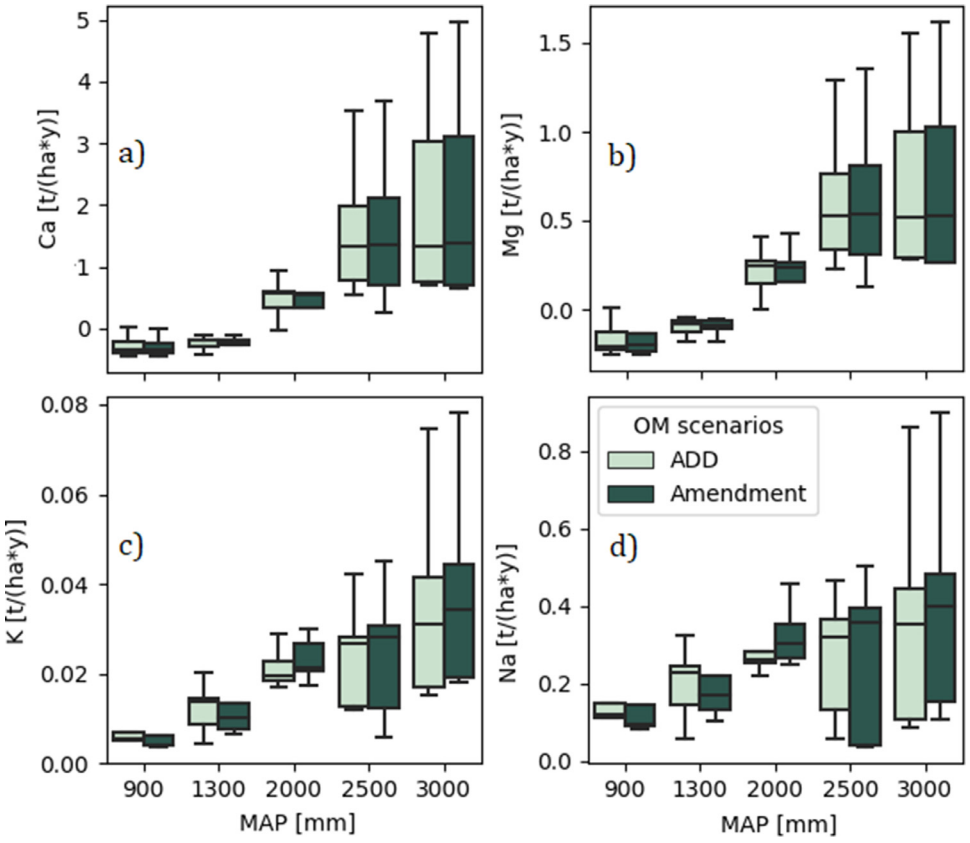

Fig. 9. Box plots related to the annual increase of calcium (a) magnesium (b), potassium (c) and sodium (d) under the considered climate scenarios and different inputs of organic matter.

olivine dissolution (i.e., HCO_3^- and CO_3^{2-}) tend to remain in solution, thus leading to carbon sequestration in aqueous form. To see significant amounts of sequestered CO_2, due to the leaching of bicarbonate and carbonate ions, much longer time scales would be necessary, especially in the condition where MAP and leaching rate are low.

3.3.2. Increase of nutrients availability

In general, olivine dissolution leads to an increase of nutrients availability in soil water (Renforth et al., 2015). Figure 9a–d show the annual increase of dissolved calcium, magnesium, potassium and sodium, respectively, for all climate scenarios. As MAP increases, in line with the increase in weathering rate (Fig. 7c), the additional availability of nutrients becomes more pronounced above 2000 mm. Even if olivine releases only magnesium from dissolution, the results show an increase of the mass of all the considered nutrients in soil water. This is related to the fact that larger magnesium concentrations in the soil solution lead to greater adsorbed amounts of this mineral on soil colloids, since the adsorption process is regulated by equilibrium reactions. As a result, magnesium replaces adsorbed calcium, sodium and potassium ions, which are thus released in the solution. In the S2 and S3 scenarios, however, there is a slight reduction of magnesium in soil water, which is due to the higher soil organic matter content and CEC, such that magnesium released by olivine dissolution ends up almost entirely adsorbed. The same behavior is observed for calcium since it has the same valence of magnesium. Due to their low adsorption processes, potassium and sodium instead tend to remain in solution.

The increase of these nutrient concentration in soil water, in response to the carbon amendment, is given by two contrasting effects on soil pH: an increase in cation exchange capacity, and a greater decomposition of carbonate and bicarbonate ions along with a higher H^+ input due to infiltration and plants action. By determining which of the two effects prevails, climate plays a very relevant role, with a more pronounced increase in nutrients only above a MAP of 2000 mm. Note that, in the long-term, olivine dissolution cases a general loss of exchangeable calcium, potassium, and sodium, since these ions are replaced by magnesium (which is continuously released from olivine dissolution). As olivine dissolves, this loss becomes progressively more relevant due to the reduction of olivine particles diameter and the corresponding increase of the weathering rate (i.e., a greater input of magnesium).

4. Conclusions

We presented a detailed analysis of EW simulations of olivine in field conditions under time varying rainfall conditions. The combination of soil, vegetation and climate conditions have been chosen with the aim of understanding the ecohydrological control on EW and, ultimately, of giving some insight into which climate (hence regions) could be more suitable for EW in current and future scenarios. The interplay between climate, organic matter, and pH is recognized as the key factors affecting for EW dynamics.

While humid climate promote faster olivine dissolution, we found that it is for MAP higher than 2000 mm that carbon sequestration increases substantially, due to the combination of higher weathering and leaching rates. However, the CO_2 sequestration rate (here computed as the leaching of the extra amounts of HCO_3^- and CO_3^{2-} produced by olivine dissolution) remains very small, emphasizing the fact that large land area is needed for EW to be effective.

Olivine application also leads to an increase of soil pH and nutrients availability in soil water, especially calcium and magnesium (at least in the short-term), which in turn can enhance plant productivity. Humid climates are again more suitable since as MAP increases and particularly when it exceeds 2000 mm, the extra masses of these nutrients provided by olivine dissolution grow as well. Furthermore, increasing the soil organic carbon content, e.g., through organic matter amendment, was not effective for both carbon sequestration and increase of nutrients availability in drier conditions (MAP lower than 2000 mm), at least for the

assumed amount of amendment. This is due to the fact that a greater organic matter concentration leads to a general growth of soil pH and a consequent decrease of weathering rate. By contrast, for more humid climates (MAP higher than 2000 mm), a greater carbon content results in a lower pH and a higher weathering rate and carbon sequestration.

Further applications of this model could explore the influence of soil properties, to identify which soil type under specific climates is more suitable toward EW applications, and the effect of rainfall seasonality on EW rates. In addition, it would be interesting to study also the liming effect of EW, due to the displacement of exchangeable Al^{3+}, and the consequent effect on soil fertility. Overall, our results suggest that details of ecohydrological variability and its impact on EW are important for a sound techno-economic analysis of EW feasibility.

Declaration of Competing Interest

The authors declare that they have no known competing financial interests or personal relationships that could have appeared to influence the work reported in this paper.

References

Allison, F.E., 1973. Chapter 7 the organic matter content of soils. In: Allison, F. (Ed.), Soil Organic Matter and Its Role in Crop Production, Vol. 3 of Developments in Soil Science. Elsevier, pp. 120–138. https://doi.org/10.1016/S0166-2481(08)70565-8. http://www.sciencedirect.com/science/article/pii/S0166248108705658

Ahrens, T.J., Lower, J.H., Lagus, P.L., 1971. Equation of state of forsterite. J. Geophys. Res. (1896-1977) 76 (2), 518–528. https://doi.org/10.1029/JB076i002p00518. https://agupubs.onlinelibrary.wiley.com/doi/abs/10.1029/JB076i002p00518

Assouline, S., 2005. On the relationships between the pore size distribution index and characteristics of the soil hydraulic functions. Water Resour. Res. 41 (7). https://doi.org/10.1029/2004WR003511. https://agupubs.onlinelibrary.wiley.com/doi/abs/10.1029/2004WR003511

Atkinson, C.J., Fitzgerald, J.D., Hipps, N.A., 2010. Potential mechanisms for achieving agricultural benefits from biochar application to temperate soils: a review. Plant Soil 337, 1–18. https://doi.org/10.1007/s11104-010-0464-5.

Baca, M.T., Fernandez-Figares, I., Mondini, C., De Nobili, M., 1996. Changes in the Amino Acid Composition of Grass Cuttings During Turned Pile Composting. Springer Netherlands, Dordrecht, pp. 1063–1066.

Cipolla, G., Calabrese, S., Noto, L.V., Porporato, A., 2021. The role of hydrology on enhanced weathering for carbon sequestration. I. Modeling rock-dissolution reactions coupled to plant, soil moisture, and carbon dynamics. Adv. Water Resour. 103934. https://doi.org/10.1016/j.advwatres.2021.103934.

D'Odorico, P., Laio, F., Porporato, A., Rodriguez-Iturbe, I., 2003. Hydrologic controls on soil carbon and nitrogen cycles. II. A case study. Adv. Water Resour. 26 (1), 59–70. https://doi.org/10.1016/S0309-1708(02)00095-7. http://www.sciencedirect.com/science/article/pii/S0309170802000957

Groshans, G.R., Mikhailova, E.A., Post, C.J., Schlautman, M.A., Cope, M.P., Zhang, L., 2019. Ecosystem services assessment and valuation of atmospheric magnesium deposition. Geosciences 9 (8). https://doi.org/10.3390/geosciences9080331.

Hartmann, J., West, A.J., Renforth, P., Köhler, P., De La Rocha, C.L., Wolf-Gladrow, D.A., Dürr, H.H., Scheffran, J., 2013. Enhanced chemical weathering as a geoengineering strategy to reduce atmospheric carbon dioxide, supply nutrients, and mitigate ocean acidification. Rev. Geophys. 51 (2), 113–149. https://doi.org/10.1002/rog.20004. https://agupubs.onlinelibrary.wiley.com/doi/abs/10.1002/rog.20004

Hegerl, G., Black, E., Allan, R., Ingram, W., Polson, D., 2015. Challenges in quantifying changes in the global water cycle. Bull. Am. Meteorol. Soc. 96 (7), 1097–1115. https://doi.org/10.1175/BAMS-D-13-00212.1.

Kopittke, P.M., Menzies, N.W., 2007. A review of the use of the basic cation saturation ratio and the "ideal" soil. Soil Sci. Soc. Am. J. 71 (2), 259–265. https://doi.org/10.2136/sssaj2006.0186. https://acsess.onlinelibrary.wiley.com/doi/abs/10.2136/sssaj2006.0186

Lasaga, A.C., 1984. Chemical kinetics of water-rock interactions. J. Geophys. Res. 89 (B6), 4009–4025. https://doi.org/10.1029/JB089iB06p04009. https://agupubs.onlinelibrary.wiley.com/doi/abs/10.1029/JB089iB06p04009

Merry, R., 2009. Acidity and alkalinity of soils. In: Sabljic, A. (Ed.), Environmental and Ecological Chemistry - Vol.II. Eolss Publisher Co. Ltd., Oxford, United Kingdom, pp. 115–131.

Mikhailova, E.A., Post, G.C., Cope, M.P., Post, C.J., Schlautman, M.A., Zhang, L., 2019. Quantifying and mapping atmospheric potassium deposition for soil ecosystem services assessment in the united states. Front. Environ. Sci. 7, 74. https://doi.org/10.3389/fenvs.2019.00074. https://www.frontiersin.org/article/10.3389/fenvs.2019.00074

Morel, F., Hering, J., 1993. Principles and Applications of Aquatic Chemistry. ISBN 0-471-54896-0

Mueller, H.J., Lathe, C., Schilling, F.R., 2005. Chapter 4 - simultaneous determination of elastic and structural properties under simulated mantle conditions using multi-anvil device max80. In: Chen, J., Wang, Y., Duffy, T.S., Shen, G., Dobrzhinetskaya, L.F. (Eds.), Advances in High-Pressure Technology for Geophysical Applications. Elsevier, Amsterdam, pp. 67–94. https://doi.org/10.1016/B978-044451979-5.50006-5. http://www.sciencedirect.com/science/article/pii/B9780444519795500065

Pelak, N., Revelli, R., Porporato, A., 2017. A dynamical systems framework for crop models: toward optimal fertilization and irrigation strategies under climatic variability. Ecol. Modell. 365, 80–92. https://doi.org/10.1016/j.ecolmodel.2017.10.003. http://www.sciencedirect.com/science/article/pii/S0304380017304325

Porporato, A., D'Odorico, P., Laio, F., Rodriguez-Iturbe, I., 2003. Hydrologic controls on soil carbon and nitrogen cycles. I. Modeling scheme. Adv. Water Resour. 26 (1), 45–58. https://doi.org/10.1016/S0309-1708(02)00094-5. http://www.sciencedirect.com/science/article/pii/S0309170802000945

Porporato, A., Rodriguez-Iturbe, I., 2013. From random variability to ordered structures: a search for general synthesis in ecohydrology. Ecohydrology 6 (3), 333–342. https://doi.org/10.1002/eco.1400. https://onlinelibrary.wiley.com/doi/abs/10.1002/eco.1400

Pulido-Villena, E., Reche, I., Morales-Baquero, R., 2006. Significance of atmospheric inputs of calcium over the southwestern mediterranean region: high mountain lakes as tools for detection. Global Biogeochem. Cycles 20 (2). https://doi.org/10.1029/2005GB002662. https://agupubs.onlinelibrary.wiley.com/doi/abs/10.1029/2005GB002662

Renforth, P., von Strandmann, P.P., Henderson, G., 2015. The dissolution of olivine added to soil: implications for enhanced weathering. Appl. Geochem. 61, 109–118. https://doi.org/10.1016/j.apgeochem.2015.05.016. http://www.sciencedirect.com/science/article/pii/S0883292715001389

Riley, W.J., Subin, Z.M., Lawrence, D.M., Swenson, S.C., Torn, M.S., Meng, L., Mahowald, N.M., Hess, P., 2011. Barriers to predicting changes in global terrestrial methane fluxes: analyses using CLM4ME, a methane biogeochemistry model integrated in CESM. Biogeosciences 8 (7), 1925–1953. https://doi.org/10.5194/bg-8-1925-2011. https://www.biogeosciences.net/8/1925/2011/

Slessarev, E.W., Lin, Y., Bingham, N.L., Johnson, J.E., Dai, Y., Schimel, J.P., Chadwick, O.A., 2016. Water balance creates a threshold in soil ph at the global scale. Nature 540, 567–569. https://doi.org/10.1038/nature20139.

Suarez, D.L., Ŝimunek, J., 1997. UNSATCHEM: unsaturated water and solute transport model with equilibrium and kinetic chemistry. Soil Sci. Soc. Am. J. 61 (6), 1633–1646. https://doi.org/10.2136/sssaj1997.03615995006100060014x. https://acsess.onlinelibrary.wiley.com/doi/abs/10.2136/sssaj1997.03615995006100060014x

Suweis, S., Rinaldo, A., van der Zee, S., Daly, E., Maritan, A., Porporato, A., 2010. Stochastic modeling of soil salinity. Geophys. Res. Lett. 37, L07404. https://doi.org/10.1029/2010GL042495.

Sverdrup, H., Warfvinge, P., 1988. Weathering of primary silicate minerals in the natural soil environment in relation to a chemical weathering model. Water Air Soil Pollut. 38, 387–408. https://doi.org/10.1007/bf00280768.

Taylor, L.L., Beerling, D.J., Quegan, S., Banwart, S.A., 2017. Simulating carbon capture by enhanced weathering with croplands: an overview of key processes highlighting areas of future model development. Biol. Lett. 13 (4), 20160868. https://doi.org/10.1098/rsbl.2016.0868. https://royalsocietypublishing.org/doi/abs/10.1098/rsbl.2016.0868

ten Berge, H.F.M., van der Meer, H.G., Steenhuizen, J.W., Goedhart, P.W., Knops, P., Verhagen, J., 2012. Olivine weathering in soil, and its effects on growth and nutrient uptake in Ryegrass (Lolium perenne L.): a pot experiment. PLOS ONE 7 (8), 1–8. https://doi.org/10.1371/journal.pone.0042098.

Weil, R., Brady, N., 2017. The Nature and Properties of Soils. 15th edition.

Weiß, M., Menzel, L., 2008. A global comparison of four potential evapotranspiration equations and their relevance to stream flow modelling in semi-arid environments. Adv. Geosci. 18, 15–23. https://doi.org/10.5194/adgeo-18-15-2008. https://www.adv-geosci.net/18/15/2008/

Zeri, M., S. Alvalá, R.C., Carneiro, R., Cunha-Zeri, G., Costa, J.M., Rossato Spatafora, L., Urbano, D., Vall-Llossera, M., Marengo, J., 2018. Tools for communicating agricultural drought over the brazilian semiarid using the soil moisture index. Water 10 (10). https://doi.org/10.3390/w10101421. https://www.mdpi.com/2073-4441/10/10/1421